THE ASTROPHYSICAL JOURNAL, 422:831–844, 1994 February 20

NON–LTE MODEL ATMOSPHERE ANALYSIS OF NOVA CYGNI 1992

P. H. HAUSCHILDT, S. STARRFIELD,[1] AND S. AUSTIN
Department of Physics and Astronomy, Arizona State University, Tempe, AZ 85287-1504
R. M. WAGNER[2]
Department of Astronomy, Ohio State University, Columbus, OH 43210
S. N. SHORE[1]
Department of Physics and Astronomy, Indiana University at South Bend, 1700 Mishawaka Avenue, South Bend, IN 46634-7111
and GHRS Science Team/CSC, Code 681, Goddard Space Flight Center
AND
G. SONNEBORN[1]
LASP, Code 681, Goddard Space Flight Center, Greenbelt, MD 20771
Received 1993 June 3; accepted 1993 August 24

ABSTRACT

We use spherically symmetric, non–LTE, line-blanketed, expanding model atmospheres to analyze the *IUE* and optical spectra of Nova Cygni 1992 during the early phases of its outburst. We find that the first *IUE* spectrum obtained just after discovery on 1992 February 20, is best reproduced by a model atmosphere with a steep density gradient and homologous expansion, whereas the *IUE* and optical spectra obtained on February 24 show an extended, optically thick, wind structure. Therefore, we distinguish two phases of the early evolution of the nova photosphere: the initial, rapid, "fireball" phase and the subsequent, much longer, optically thick "wind" phase. The importance of line-blanketing in nova spectra is demonstrated. Our preliminary abundance analysis implies that hydrogen is depleted in the ejecta, corresponding to abundance enhancements of Fe by a factor of ≈ 2 and of CNO by more than a factor of 10 when compared to solar abundances. The synthetic spectra reproduce both the observed pseudo-continua as well as most of the observed features from the UV to the optical spectral range and demonstrate the importance of obtaining nearly simultaneous UV and optical spectra for performing accurate analyses of expanding stellar atmospheres (for both novae and supernovae).

Subject headings: novae, cataclysmic variables — stars: abundances — stars: atmospheres — stars: individual (Nova Cygni 1992) — ultraviolet: stars

1. INTRODUCTION

Nova Cygni 1992 (hereafter, NCyg92) was discovered in outburst on 1992 February 19.07 UT (Collins 1992). Thanks to electronic mail, notification of this discovery was extremely fast, and we were able to obtain optical and ultraviolet spectra for this nova at intervals of a few days, or less, during the critical first weeks of the outburst. In particular, we were able to observe the initial stages of the expansion when the nova was optically thick in both the lines and the continuum. This "fireball" stage has never before been observed in the ultraviolet.

The importance of this observation cannot be overemphasized because the spectral features in the fireball phase give us information on the velocity field imposed on the ejecta at the beginning of the explosion. The velocity field, in turn, provides us with a detailed view of how the material was ejected. By the time the nebular spectrum has been detected, most of the important information about the most rapidly expanding material is no longer available. This is because the emission measure of this gas decreases very quickly. It is only in the first few days, when the lines are still optically thick and display P Cygni profiles, that a full picture of the shell dynamics can be obtained. It is this information that helps determine the kinetic energy of the ejecta and that also places limits on the roles of the two competing ejection mechanisms, shock versus wind acceleration. This fireball stage also gives us information about the overall mixing of the ejected material. It is thus very significant that we have finally obtained this information for a nova, especially since NCyg92 was an ONeMg nova.

In this paper, we first present an analysis of the optical and ultraviolet line profiles using a full dynamical non–LTE atmosphere code. During the early phases the UV spectra are characterized by the simultaneous presence of absorption, P Cygni, and emission features. In order to model the early spectra of NCyg92, we have included (*a*) non–LTE effects, (*b*) line-blanketing by UV metal lines, in particular Fe II, (*c*) proper treatment of the radiative transfer for lines and continua, and (*d*) a self-consistent solution of the radiative energy equation (i.e., radiative equilibrium in the comoving frame).

We first describe the observational data used in the subsequent analysis (§ 2). Next in § 3, we briefly describe the numerical method used to analyze the observed spectra. In § 4 we compare the observed to the synthetic spectra and discuss the parameters of the model atmospheres. We end with a summary and discussion.

2. OBSERVATIONS

We have obtained high-resolution spectra of NCyg92, from its discovery, with both the long-wavelength primary (LWP; 2000–3300 Å) and short-wavelength primary (SWP; 1175–

[1] Guest Investigator, *IUE* Observatory.
[2] Current postal address: Lowell Observatory, 1400 W Mars Hill Road, Flagstaff, AZ 86001.

1950 Å) cameras of the *International Ultraviolet Explorer* satellite (*IUE*). These were obtained in both high- and low-resolution modes and they are described more thoroughly in the companion papers (Shore et al. 1993, 1994). All *IUE* spectra have been reduced at the GSFC Regional Data Analysis Facility (RDAF) using standard *IUE* software and special purpose IDL routines (see Shore et al. 1993).

We followed the optical spectrophotometric development of NCyg92 using the Ohio State University CCD spectrograph on the Perkins 1.8 m telescope of the Ohio Wesleyan and Ohio State Universities at the Lowell Observatory. Spectra were obtained on a weekly basis starting 4 days after discovery and continuing through June, and then at monthly intervals thereafter until 1993 May. Our spectra covered the wavelength range from 3300 Å to 8500 Å with the most consistent coverage from 4500 Å to 5700 Å. Most spectra were obtained with 4 Å resolution. The optical spectra were reduced using standard IRAF procedures (Wagner 1992).

We have detected significant changes in the structure of the expanding material over the first few days of the outburst and concentrate in this paper on an analysis of the spectra from this time. In this section we present representative *IUE* spectra from the first few days of the outburst. We find that the appearance of the initial spectrum is unique. We then show the changes that occurred over the first few days of the outburst and, finally, compare the spectra of NCyg92 to archival data for one of the two other slow ONeMg novae with spectra in the *IUE* archives, QU Vul 1984.

NCyg92 was discovered in outburst at a visual magnitude of 6.8 on 1992 February 19.07 (Collins 1992). He waited one full day in order to confirm his discovery and the announcement was not made until February 20. The nova did not reach optical maximum ($V = 4.4$) until February 24.170 (Mikuz 1992). Our *IUE* observations were begun shortly after the report of the discovery reached us as a result of an accepted *IUE* Target-of-Opportunity Bright Nova proposal. We state this to emphasize that the results of this paper would have been impossible to obtain without the flexibility of *IUE* scheduling and operations. Figure 1 shows three different SWP spectra of NCyg92. The solid line is our first spectrum, which was obtained on 1992 February 20.9 (SWP 44030; low resolution, large aperture; 9.7 s). It is completely unlike any previous ultraviolet spectrum of a nova in outburst. There is flux detectable at all wavelengths but the only feature that can be positively identified is Al III λ1858 Å which exhibits a deep P Cygni profile. The only emission line positively identifiable in the LWP spectra is Mg II 2800 Å, and it also shows a P Cygni profile. The blueward extension of the profiles on the high-dispersion spectra reached velocities of *at least* 3000 km s^{-1}.

We also display two more spectra in Figure 1. The dotted line is a spectrum (SWP 44031; low dispersion; large aperture; 44 s) that was taken about 50 minutes after the first spectrum and which displays measurable differences over this time period. The correspondence of structure between these two spectra shows that most of the features are real and the product of numerous broad, overlapping, iron peak lines (we justify this statement in the next section). The final spectrum is shown near the bottom of the plot and was obtained 1 day later (SWP 44040; low dispersion, large aperture; 420 s). We show it to demonstrate the rapidity with which the flux had dropped in the short-wavelength region of the spectrum. The integrated flux had fallen by more than a factor of 10 within this 24 hr period. This last spectrum is more typical of the early spectra of novae (Hauschildt et al. 1992). Note the almost complete absence of detectable flux below 1600 Å.

The development and cause of this rapid decline is discussed

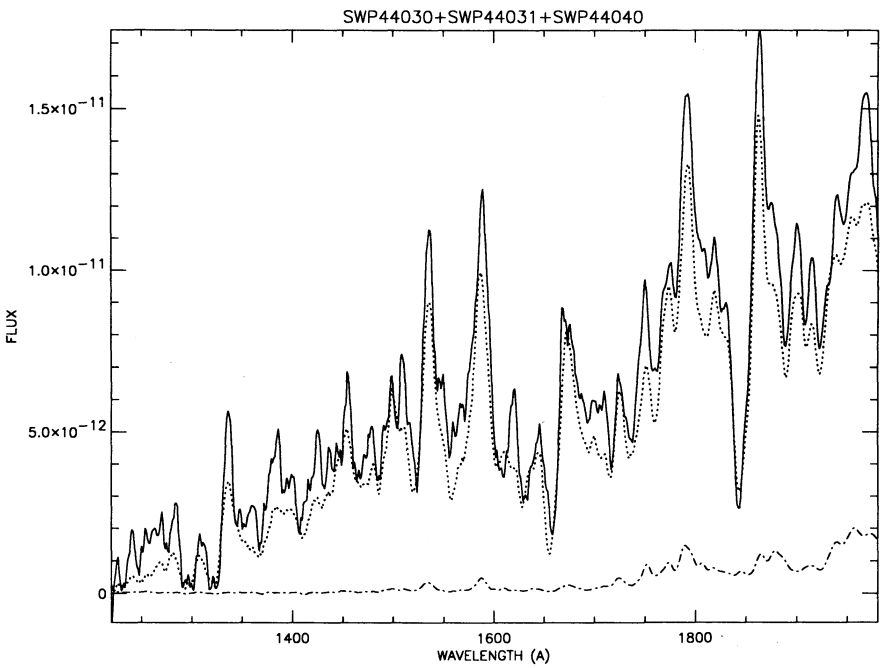

FIG. 1.—This plot shows three of the first ultraviolet spectra, obtained with the *IUE* satellite, for Nova Cygni 1992. SWP 44030 (*solid line*) was our first spectrum, obtained before the expanding shell reached optical maximum. SWP 44031 (*dotted line*) was obtained ~1 hr later and shows that the flux was decreasing in the UV. Note the great depth of the P Cygni profile of Al III 1860 Å. As the ejecta continue to expand and cool, SWP 44040 (*dash-dot line*) shows that the flux has dropped by a factor of 10 over a 1 day interval. All spectra are de-reddened by $E(B-V) = 0.3$. Note that there is detectable flux at all wavelengths in the first spectrum.

in more detail in Shore et al. (1993, 1994). Here, we just briefly mention that we interpret these spectra to imply that we have caught a nova for the first time in the UV in the "fireball" phase. This is the stage when the hot, dense, material that has just been ejected from the white dwarf is expanding adiabatically and cooling. Over the first few hours, the expanding layers cool further so that the peak of the emitted energy moves into the optical spectral range and the UV flux continues to decline. Once optical maximum is reached, the declining density causes the region where the continuum is formed to move inward in mass, toward denser, hotter, regions. The color temperature of the pseudo-continuum then begins to increase and the flux peak moves back into the ultraviolet.

This can be seen in Figure 2, which shows how the ultraviolet flux recovered over a 3 day interval. The lower spectrum was obtained on 1992 February 26.1 (SWP 44060; low dispersion; large aperture; 49.8 s) and the upper spectrum on 1992 February 27.9 (SWP 44073; low dispersion; large aperture; 39.6 s). For comparison, in Figure 3 we show two early ultraviolet spectra of QU Vul which was also a slow ONeMg nova (SWP 24795; low dispersion, large aperture, 1200 s; 1 January 1985 and SWP 24862; low dispersion, large aperture, 900 s; 1985 January 8). The comparison should be restricted to the region from 1230 Å to about 1750 Å since the peaks at longer wavelengths on the QU Vul spectrum were all overexposed. Unfortunately, there are no spectra of QU Vul in the early outburst that are not overexposed from about 1700 Å to the red edge of the wavelength range. The similarity between these two novae is obvious. The point we are emphasizing, however, is that it was the spectra obtained *after recovery from the deep minimum in ultraviolet flux* (Shore et al. 1994b) that exhibited those features that we had previously thought were characteristic of a nova at the *beginning* of the outburst. We also note that except for Al III 1858 Å, many of the other emission peaks are actually regions of transparency between overlapping (mostly Fe II) lines.

As the nova evolves in time, the density of the optically thin layers decreases and the pseudo-photosphere continues to move inward in mass to deeper and hotter layers. This continues until Fe II begins to ionize and the opacity begins to decrease. The deep minima in these spectra at around 1700 Å, where the opacity is highest, begin to move upward in flux and the contrast between the peaks and valleys decreases. We refer to this as the lifting of the iron curtain. The transparency of the outer layers increases until the pseudo-continuum of overlapping lines finally disappears and we are left with the collisionally excited nebular emission lines. A discussion of this stage is given in Shore et al. (1993).

In summary of this section, we find that we have caught this nova at a unique (with respect to all other novae studied with *IUE*) time in its evolution; the fireball stage, when the expanding, optically thick, outer layers of the ejecta have not yet reached their maximum extent. As they expand and cool, the ultraviolet flux declines by more than a factor of 10 in 1 day. Subsequent to optical maximum, the ultraviolet flux recovers to values similar to those obtained when first discovered but the entire character of the spectrum has changed. Our model atmosphere analysis of these first spectra and the physical basis of the statements made in this section are given in the succeeding sections of this paper.

3. MODEL ATMOSPHERES

3.1. *Model Construction*

The spectral synthesis of the early spectra of NCyg92 was done using a method similar to that described by Hauschildt et al. (1992). Therefore, we provide only a brief description of the

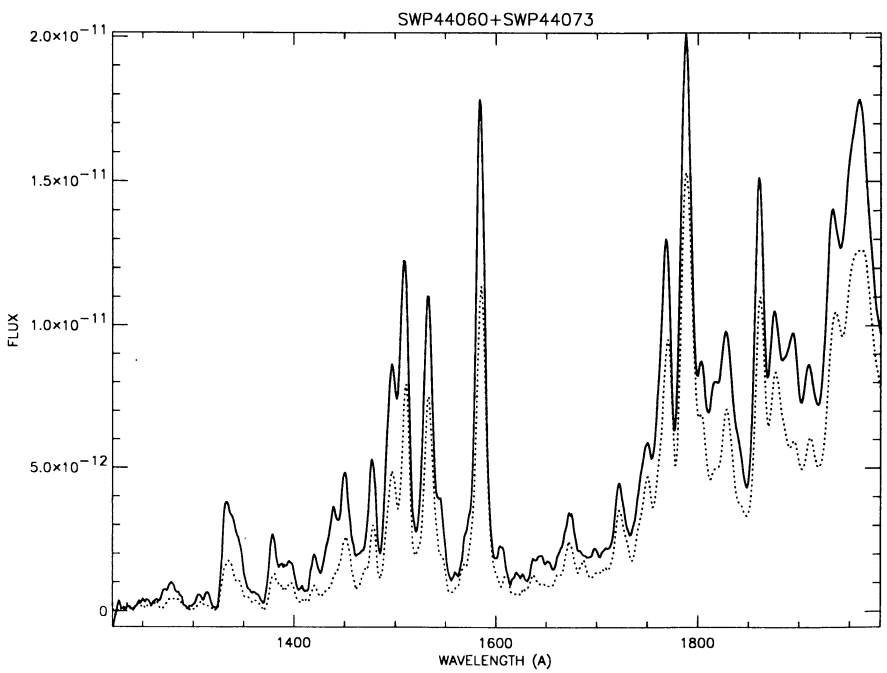

FIG. 2.—These two spectra show the recovery from the deep minimum in the UV light curve (Shore et al. 1994). They have been dereddened by $E(B-V) = 0.3$. SWP 44060 (*dotted line*) was obtained 5 days after the last spectrum shown in Fig. 1. The peak flux has started to move back into the UV. Virtually all of the features present in the spectrum (except for Al III 1860 Å) are regions of transparency between overlapping iron lines and not emission lines. SWP 44073 (*solid line*) was obtained 1 day after 44060.

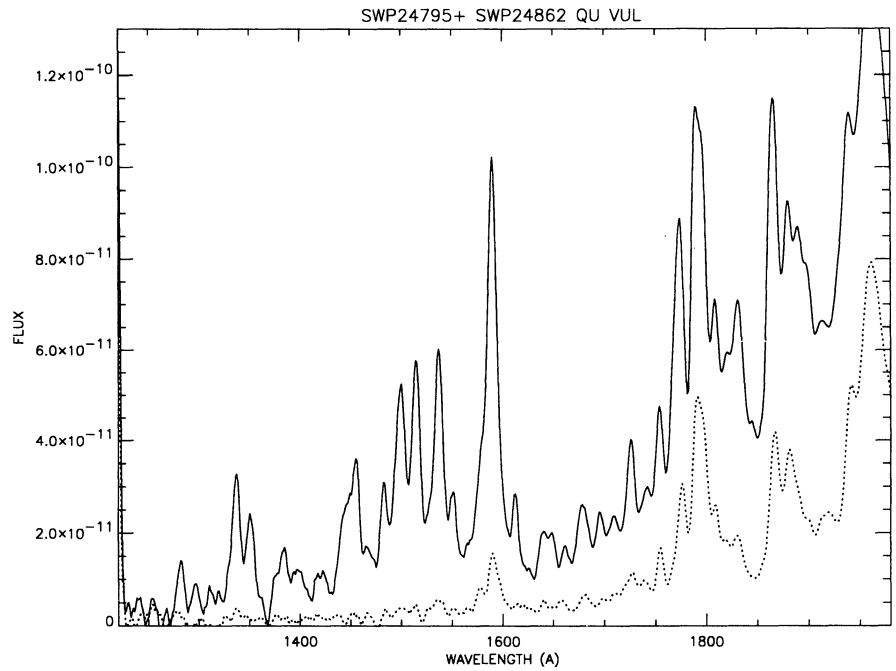

FIG. 3.—In this plot we show two spectra of QU Vul 1984, another slow ONeMg nova. They have been dereddened by $E(B-V) = 0.6$ (Saizar et al. 1992). SWP 24795 (*dotted line*) was obtained on 1985 January 1, a few days after discovery. It shows virtually no detectable flux below about 1500 Å and closely resembles SWP 44060. SWP 24862 (*solid line*) was obtained on 1985 January 8 and shows how the features from 1400 Å to 1600 Å grow in strength over time. We have deliberately allowed the peaks of the lines longward of 1800 Å to extend above the plot because they are overexposed. We are more interested in showing the general similarities of the spectra than a detailed comparison of every feature.

method and summarize the recent changes to Hauschildt's non–LTE, expanding stellar atmosphere code PHOENIX.

PHOENIX solves the special relativistic equation of radiative transfer (SSRTE) in the Lagrangian frame self-consistently with the multilevel, non–LTE rate equations and the special relativistic radiative equilibrium (RE) equation in the Lagrangian frame. The version of PHOENIX described by Hauschildt et al. (1992) for nova atmosphere calculations used the Discrete Ordinate Matrix Exponential (DOME) method (Hauschildt & Wehrse 1991) for the solution of the SSRTE as well as the RE condition and the Equivalent-Two-Level-Atom (ETLA) method (e.g., Mihalas 1978) for the consistent solution of the multilevel non–LTE rate equations. Recent improvements to PHOENIX include the following: (i) the numerical solution of the SSRTE is done using the Accelerated Lambda Iteration (ALI) method described by Hauschildt (1992a), (ii) the RE equation is solved by the hybrid (ALI combined with partial linearization) method given by Hauschildt (1992b), and (iii) the multilevel non–LTE continuum and line transfer problem is treated using the ALI method described by Hauschildt (1993). These methods greatly improve the numerical stability and the performance of PHOENIX and were used for the computation of all atmosphere models and synthetic spectra shown here.

We treat the following species in non–LTE: H I with 10 levels, Mg II with 3 levels, and Ca II with five levels (see Hauschildt et al. 1992 for details). The Mg II model atom is necessary to calculate the formation of the $h + k$ lines, and the Ca II model atom is sufficient for the calculation of the H + K lines and the Ca II infrared triplet. The lines are represented by depth-dependent Gaussian profiles with 25 wavelength points per permitted non–LTE line.

In addition to the non–LTE lines, the models include, self-consistently, line blanketing of the most important ($\approx 10^5$) metal lines selected from the line list of Kurucz & Peytremann (1978) with an updated Fe II line list (Kurucz 1988). The entire list contains close to two million lines; however not all of them are important for the case at hand. Therefore, before every temperature iteration, a smaller list is formed from the original list. First, an optical depth point is chosen, usually at $\tau_{\rm std} \approx 0.01$. Then, using the density and temperature for this point the absorption coefficient in the line center, κ_l, is calculated for every line and compared to the corresponding continuum absorption coefficient, κ_c. A line is transferred to the "small list" if the ratio κ_l/κ_c is larger than a prespecified value of Γ (usually 10^{-4}). In the subsequent radiative transfer calculations, all lines selected in this way are taken into account as individual lines, all others from the large line list are neglected. This selection procedure is repeated at *every* iteration in order to always include the most important lines, even if the temperature stratification changes significantly. We treat line scattering in the metal lines (approximately) by parameterizing the albedo for single scattering, α. The calculation of α would require a full non–LTE treatment of *all* lines and continua, which is outside of the scope of this paper. Tests have shown that, as a direct result of the velocity gradient in nova photospheres, the shape of the lines does not depend sensitively on α and our approach is a reasonable first approximation. Therefore, we adopt an average value of $\alpha = 0.95$ for all metal lines. The continuous absorption and scattering coefficients are calculated using the species and cross sections as described in Hauschildt et al. (1992).

3.2. *The Model Parameters*

The model atmospheres are characterized by the following parameters (see Hauschildt et al. 1992 for details): (i) the refer-

ence radius R, which is the radius where either the continuum optical depth in absorption or extinction at 5000 Å is unity, (ii) the effective temperature $T_{\rm eff}$, which is defined by means of the luminosity, L, and the reference radius, R, [$T_{\rm eff} = (L/4\pi R^2\sigma)^{1/4}$ where σ is Stefan's constant], (iii) the density parameter, N, [$\rho(r) \propto r^{-N}$], (iv) the maximum expansion velocity, v_∞, (v) the density, $\rho_{\rm out}$, at the outer edge of the envelope, (vi) the metal line threshold ratio, Γ, (vii) the albedo for line scattering (metal lines only, here set to 0.95), (viii) the statistical velocity ξ, treated as depth-independent isotropic turbulence, and (ix) the elemental abundances.

We emphasize that for extended model atmospheres one should not assign, a priori, a physical interpretation to the parameter combination of $T_{\rm eff}$ and R. While $T_{\rm eff}$ has a well-defined physical meaning for plane-parallel stellar atmospheres, its definition for extended atmospheres is connected to the particular definition of the radius R (see Baschek, Scholz, & Wehrse 1991). In addition, the reference radius R in our models is defined using a prescribed *continuum* optical depth scale at $\lambda = 5000$ Å and is not directly comparable to observationally derived radii. Therefore, the effective temperature is not well-defined for extended atmospheres and must be regarded only as a convenient numerical parameter.

4. RESULTS

The early UV spectra of novae are dominated by many overlapping lines of, mostly, Fe II (Hauschildt et al. 1992). This is also true for the spectra of NCyg92 which were presented in § 2. We, therefore, give here a detailed description of the effects of line blanketing in nova atmospheres before we discuss the analysis of the observed NCyg92 spectra. A discussion of the line blanketing in nova atmospheres is of general interest and applies to some extent also to supernova atmospheres.

4.1. *Line Blanketing*

In Figure 4 we show the effects of gradually increasing metal line blanketing on the UV spectra of novae for two model atmospheres with a luminosity of $L = 20{,}000\ L_\odot$ and the effective temperatures 15,000 K and $T_{\rm eff} = 25{,}000$ K. The temperature structures used to compute the synthetic spectra were taken from a fully converged non–LTE, expanding ($v_{\rm max} = 2000$ km s^{-1}), line-blanketed model atmosphere with $\Gamma = 10^{-3}$ (about 10^5 lines). The top panels show the energy distribution when only non–LTE lines are included in the calculation. In the following panels (top to bottom) the number of lines included in the synthetic spectra is increased by a factor of about 10, respectively. The dotted lines show, in each panel, the blackbody energy distribution for $T = T_{\rm eff}$.

These figures show the dramatic effect of increasing line blanketing on the UV spectra of novae. For $T_{\rm eff} = 15{,}000$ K, practically all lines are in absorption and, due to the velocity field, overlap strongly. The resulting pseudo-continuum displays the typical "emission" features which can now be identified as regions of transparency, e.g., the prominent and ubiquitous feature at $\lambda \approx 1600$ Å. For $T_{\rm eff} = 25{,}000$ K, the lines show partly P Cygni type structures but most of the lines are in absorption. Now the net effect of line blanketing (for a given temperature structure) on the spectrum is smaller, but its effect on the temperature structure is still large.

Of particular interest is the behavior of the Mg II $h + k$ lines (cf. Fig. 4*c*). For a model atmosphere with $T_{\rm eff} = 10{,}0000$ K, neglecting the blending with Fe II lines, the doublet shows a P Cygni profile. However, the blending with Fe II lines dramatically changes the appearance and the $h + k$ lines now exhibit a P Cygni profile with a relatively stronger emission component and both the red and the blue parts of the line profile have changed significantly. The model atmosphere with $T_{\rm eff} = 15{,}000$ K shows a somewhat similar behavior, but now the $h + k$ profile changes from P Cygni (no blending) to a pronounced double-peak structure characteristic of novae at this stage.

These combined effects demonstrate the importance of line blanketing in the interpretation of early nova spectra. With increasing effective temperatures and decreasing density of the expanding shell (i.e., increasing time), line blanketing becomes less and less important and finally the nebular stage of the nova spectrum is dominated by forbidden lines.

4.2. *The First IUE Spectrum of 1992 February 20*

As discussed in § 2 the first *IUE* spectrum of NCyg92 (1992 February 20; SWP 44030 and LWP 22425) is very different from typical (early) nova spectra. The significant change of the spectrum in a very short time interval also indicates the peculiar nature of this nova spectrum. The observed spectra we display in this section have been dereddened using $E(B-V) = 0.3$ (Austin et al., in preparation).

The density structure found necessary in our earlier studies to reproduce the typical early nova spectra can be approximated by a power law $\rho \propto r^{-N}$ with $N \approx 3$ (cf. Hauschildt et al. 1992). This very shallow density law is roughly valid during the phase of constant bolometric luminosity of the nova evolution. In addition, the velocity law inside the expanding shell should correspond to a radius-independent mass-loss rate $\dot{M}$, which results in a velocity law of the form $v(r) \propto r^{N-2}$. For $N = 3$ this corresponds to a linear velocity law, which is consistent with a freely (homologously) expanding shell.

Attempts to reproduce the first *IUE* spectrum of NCyg92 using a shallow $N \approx 3$ density structure were unsuccessful. In Figure 5*a* we show the best fit we found using a $N = 3$ density structure ($T_{\rm eff} = 11{,}000$ K and $v_{\rm max} = 3000$ km s^{-1}). The slope of the (pseudo) continuum is too steep and the lines and features in the observed spectrum are significantly broader than the features seen in the synthetic spectrum. This indicates that the velocity gradient in the line-forming region is larger than the velocity gradient present in the line-forming region of the $N = 3$ model atmosphere. On the other hand, the shell at this early stage should be expanding freely and a linear velocity law should be a good assumption. We have, therefore, tried model atmospheres with much steeper density laws but kept the linear velocity law. In Figure 5*b* we show the best-fitting synthetic spectrum we found using steeper density laws. The maximum expansion velocity of the model atmosphere is $v_{\rm max} = 4500$ km s^{-1} and the density exponent is $N = 15$, corresponding to a relatively thin shell. For N as large as 15, the condition $\dot{M} = $ const. would lead to a very steep velocity gradient in the photosphere, $v(r) \propto r^{13}$. This implies too small a velocity in the deeper layers of the photosphere where many lines and the continuum is formed. Therefore, we find that the model atmosphere with $T_{\rm eff} = 11{,}000$ K, $N = 15$ and a linear velocity law is the best-fitting model for the *IUE* spectrum of February 20.

In the LWP wavelength range the agreement between the synthetic spectrum and the observation is satisfactory. In particular, the structure around the $h + k$ lines is well reproduced. However, the emission feature around 2680 Å is too strong. This feature is actually a gap in the Fe II line curtain (see also

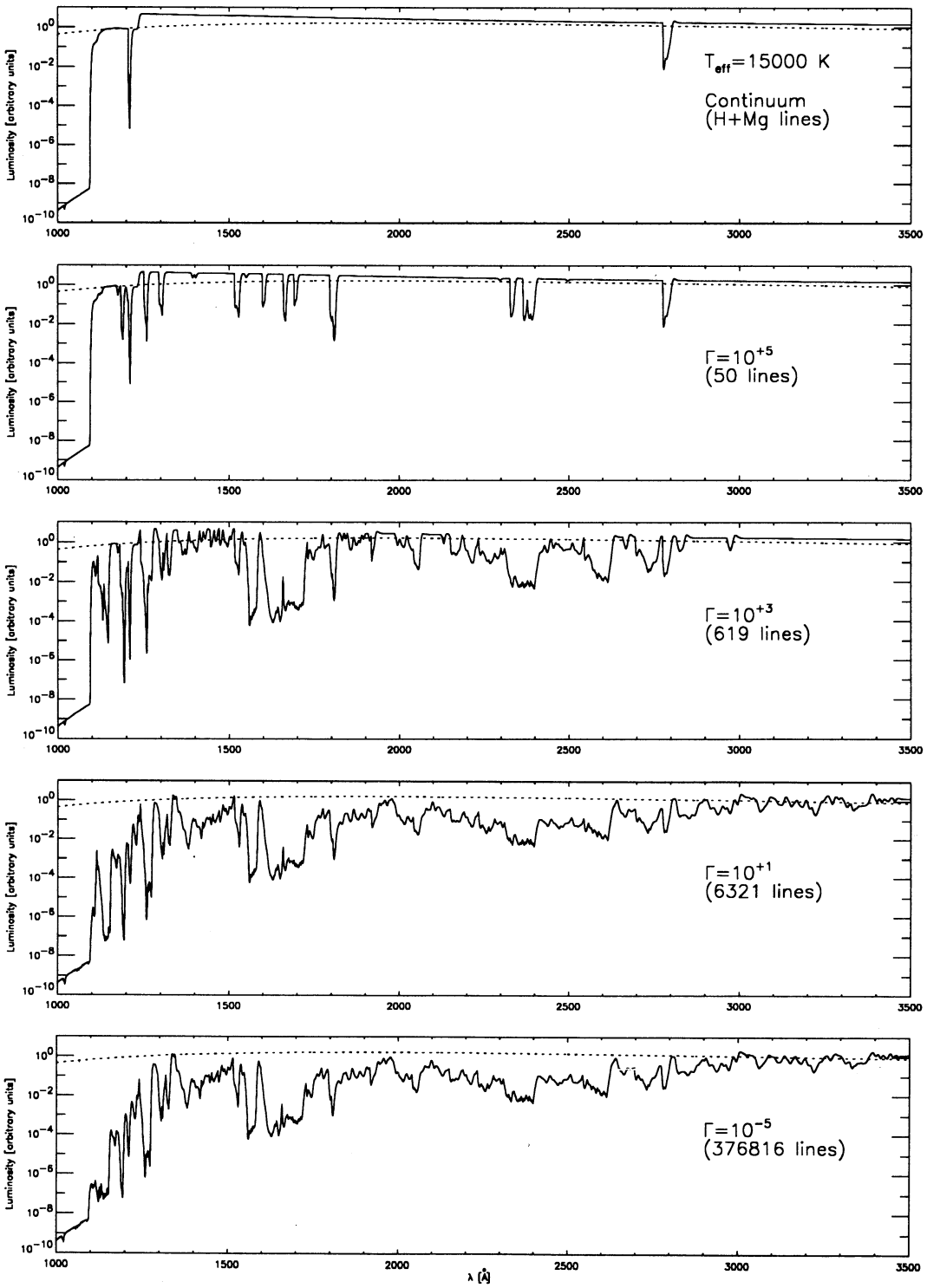

FIG. 4*a*

FIG. 4.—The effect of steadily increasing the line blanketing on synthetic nova spectra. The expanding, non–LTE model atmospheres have the common parameters $L = 20{,}000\ L_{\odot}$, $N = 3$, $v_{max} = 2000$ km s^{-1}, and solar abundances. The effective temperatures are $T_{eff} = 15{,}000$ K (*a*) and $T_{eff} = 25{,}000$ K (*b*). The calculation of the model atmosphere includes, self-consistently, non–LTE effects of H, Mg II, and Ca II (with 25 wavelength points per permitted line for each model atom) as well as line blanketing of approximately 100,000 metal lines.

For both effective temperatures, we display in the uppermost panel synthetic UV spectra in which only the non–LTE lines (H I Lyman series and the Mg II $h + k$ doublet) have been included. The dotted line gives the blackbody energy distribution for $T = T_{eff}$. The subsequent panels show synthetic spectra with an increasing number (roughly by a factor of 10 from panel to panel) of metal lines. The number of included metal lines is listed in each panel. These lines overlap strongly due to the differential expansion and form a "pseudo-continuum" (or the "iron curtain"). The figure shows the importance of an adequate treatment of metal line blanketing in modeling nova spectra during the early stages. Typically, 10^5 lines are required and sufficient for accurate model construction and a synthetic spectrum.

In (*c*) we display the region around the Mg II $h + k$ lines for two models with $T_{eff} = 10{,}000$ K (*upper panel*) and $T_{eff} = 15{,}000$ K (*lower panel*). The dotted curves give the spectrum obtained if line blanketing by Fe II lines is neglected; the full curves give the synthetic spectra including Fe II line blanketing in addition to the Mg II lines. The significant changes of the Mg II $h + k$ line profiles due to overlapping Fe II lines is very apparent in this plot and demonstrates the importance of a proper treatment of overlapping lines in the model construction and the computation of synthetic spectra of novae.

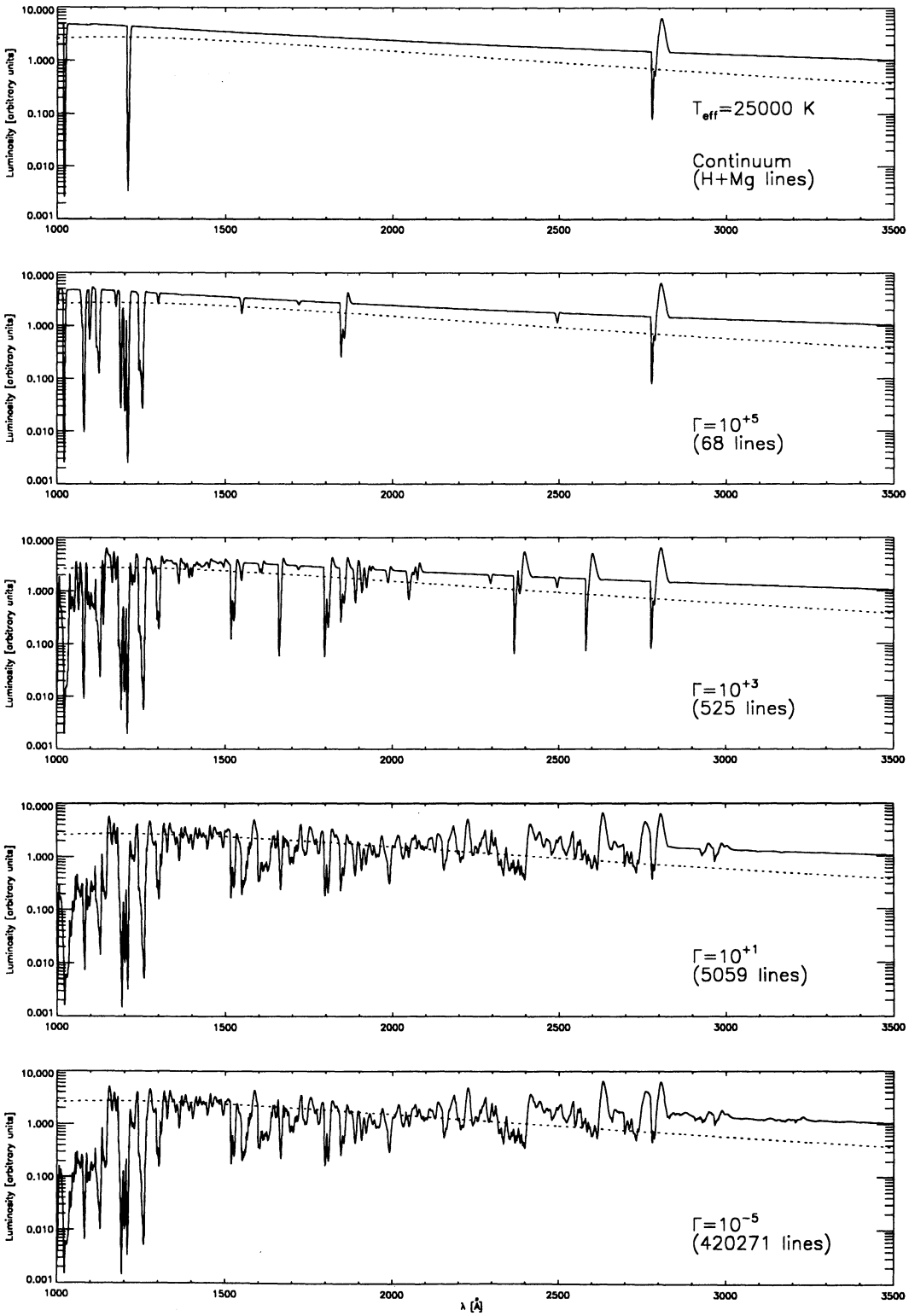

FIG. 4*b*

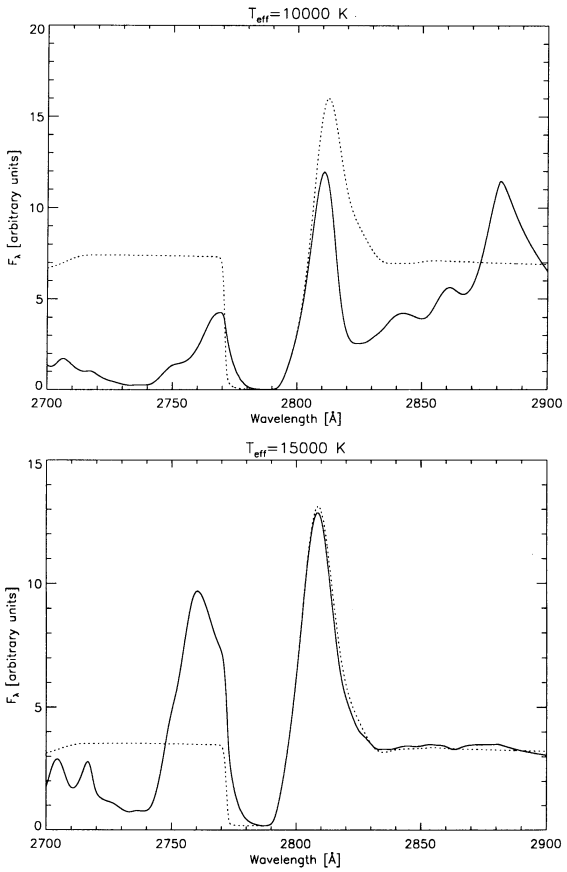

FIG. 4c

Fig. 11). In the SWP range the differences between the synthetic and observed spectra are larger. The model predicts too large a flux in the wavelength range from 1300 Å to 1600 Å and several lines between 1700 Å and 1900 Å are not reproduced. Note, however, that the spectrum between 1800 Å and 1950 Å is overexposed.

Adopting the model atmosphere used in Figure 5*b* as the best-fitting model, we have performed a preliminary abundance analysis, considering only the elements C, N, O, and Fe. Unfortunately, neon does not have strong permitted lines which would be prominent in the optical or UV spectral ranges during these early stages and could be used for a neon abundance determination. The strong Mg II $h + k$ lines are saturated although the departure coefficient of the ground state of Mg II is much smaller than unity, leading to a strong overionization of Mg II to Mg III as compared to the LTE value. An abundance analysis of Mg based on the $h + k$ lines *alone* would, therefore, be very inaccurate.

Our preliminary results show evidence for hydrogen depletion, resulting in enhanced abundances of iron (about a factor of 2) and CNO (at least a factor of 10). Changing the model abundances to these values considerably improves the fit in the SWP range. To demonstrate this, we compare in Figure 6 the *IUE* spectrum of 20 February to a synthetic spectrum computed using the same model atmosphere we used for the fit in Figure 5*b* but with the CNO abundances enhanced by a factor of 10 and the Fe abundance enhanced by a factor of 2 as compared to solar abundances.

The increased CNO abundances change the synthetic spectrum significantly in the spectral range between 1300 and 1600 Å where the opacity due to overlapping CNO lines is relatively large. Previously, the agreement between the observed and synthetic spectrum was not as good as in the other parts of the UV spectrum. The higher Fe abundance improves the overall fit to the SWP spectrum. The differences in the 1300–1600 Å wavelength range are now much smaller when compared to Figure 5*b* and the feature at about 1950 Å is well reproduced. However, the fit to the Mg $h + k$ doublet is worse. This is due to the fact that the wings of the $h + k$ lines are strongly blended with Fe II lines (cf. Fig. 3).

Hydrogen depletion is a direct prediction of the theory (Starrfield 1989). First, during the thermonuclear runaway (TNR), hydrogen is converted to helium and, correspondingly, the hydrogen abundance is lower than its initial value. In addition, mixing with metal-rich material from the white dwarf will enhance the metal abundances as compared to the hydrogen abundance. That significant mixing has occurred is evident in the identification of NCyg92 as an ONeMg nova. The CNO abundances also seem to be more enhanced when compared to the iron (or overall metal) abundance. This is caused by the nonequilibrium nuclear burning during the TNR, and is predicted by hydrodynamic models of the nova outburst.

4.3. *The Spectrum of 1992 February 24/25*

In Figure 7 we display the combined *IUE* and optical spectra of 1992 February 24 (full line) overlaid with a synthetic spectrum ($T_{\rm eff}$ = 14,000 K, $v_{\rm max}$ = 3000 km s^{-1}, N = 3, $\dot{M}$ = const, solar abundances-*dotted line*). Note that this spectrum was obtained after the recovery from the deep minimum in the UV flux (Fig. 2). This figure shows that a model atmosphere with a much shallower density gradient, N = 3, is now able to reproduce the observed spectrum over a large wavelength and flux range. In general, the slope of the pseudo-continuum is well fitted by the synthetic spectrum, but some features are again not well reproduced. The deviations in the wavelength range from 1800 Å to 1900 Å could be caused by the use of solar abundances for CNO and/or the relatively small dynamical range of the *IUE* satellite, but in order to investigate this point in greater detail, we would need UV spectra with a higher dynamical range.

In Figure 8 we show the optical spectrum together with the (solar abundance) synthetic spectrum at an expanded wavelength scale. The most important optical lines are labeled at their rest wavelength. In fact, an Fe/H ratio of twice solar results in a better overall agreement (cf. Fig. 9). This is consistent with the iron abundance we found necessary to improve the agreement between theory and observation for the first *IUE* spectrum. Because we are looking at different material, this indicates a hydrogen depletion throughout the entire envelope. The synthetic spectrum fits the observed continuum and the line profiles very well. The height of the emission part of Hβ is a few percent too small and it is somewhat redshifted in comparison to the observed spectrum. The absorption part is weaker in the observed than in the synthetic spectrum. These discrepancies could have several causes, e.g., (i) effects of nonsphericity, (ii) deviations from the assumed power-law density, (iii) contributions from the more complex absorption systems frequently found in novae, which are not resolved at the resolution of our optical spectra, and (iv) the absorption part of the profile may be filled by circumstellar emission. Definitive confirmation of the nonspherical nature of NCyg92 was reported by Shore et al. (1993) but these effects mostly modify,

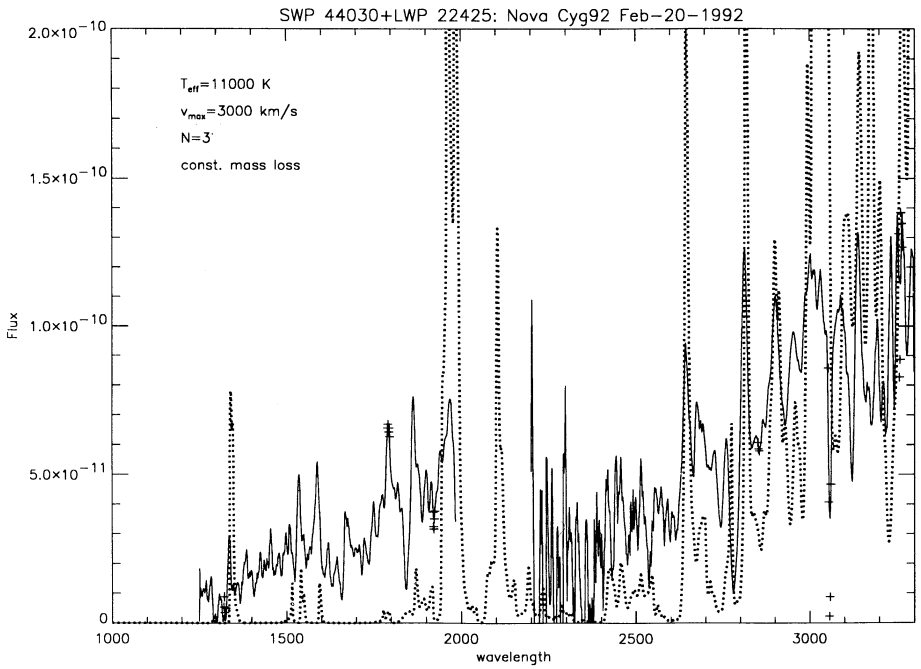

FIG. 5*a*

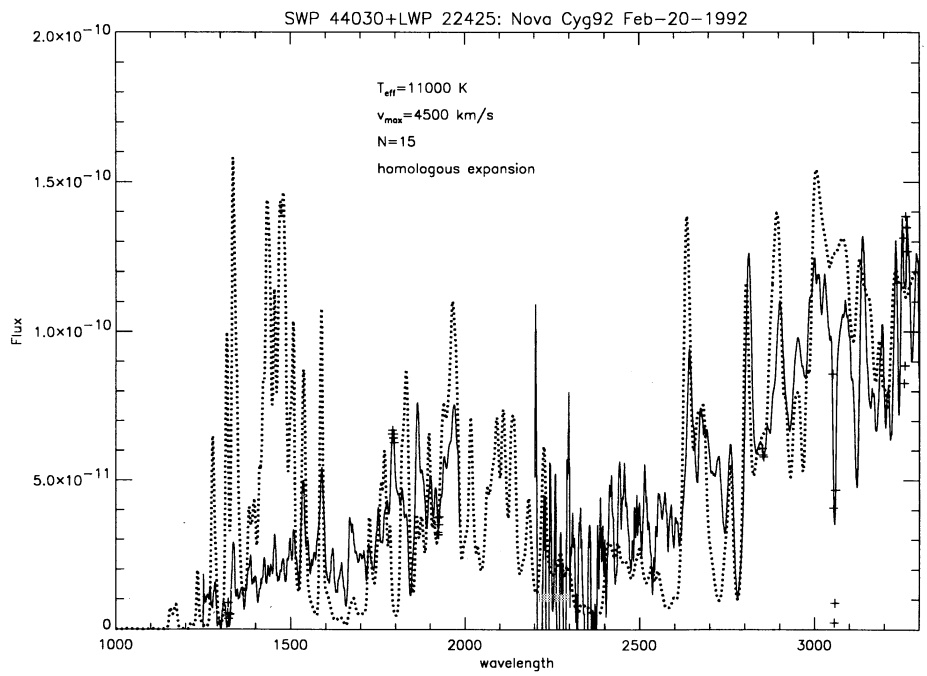

FIG. 5*b*

FIG. 5.—Comparison between the first *IUE* spectrum of NCyg92 on 1992 February 20 (*full curve*) and a synthetic spectrum computed using solar abundances (*dotted curve*). Both panels show models with the parameters $T_{\rm eff} = 11{,}000$ K, $L = 20{,}000\ L_{\odot}$, solar abundances and a linear (homologous) velocity law $v \propto r$. However, (*a*) shows a model atmosphere with a shallow density gradient $N = 3$, whereas (*b*) shows the best-fitting model atmosphere displaying a steep density gradient $N = 15$. For the first model atmosphere, the linear velocity law also leads to a radius independent mass-loss rate $\dot{M}$. The graph shows that the first spectrum of NCyg92 cannot be fitted by a typical shallow density structure normally used to do spectral analysis of nova shells.

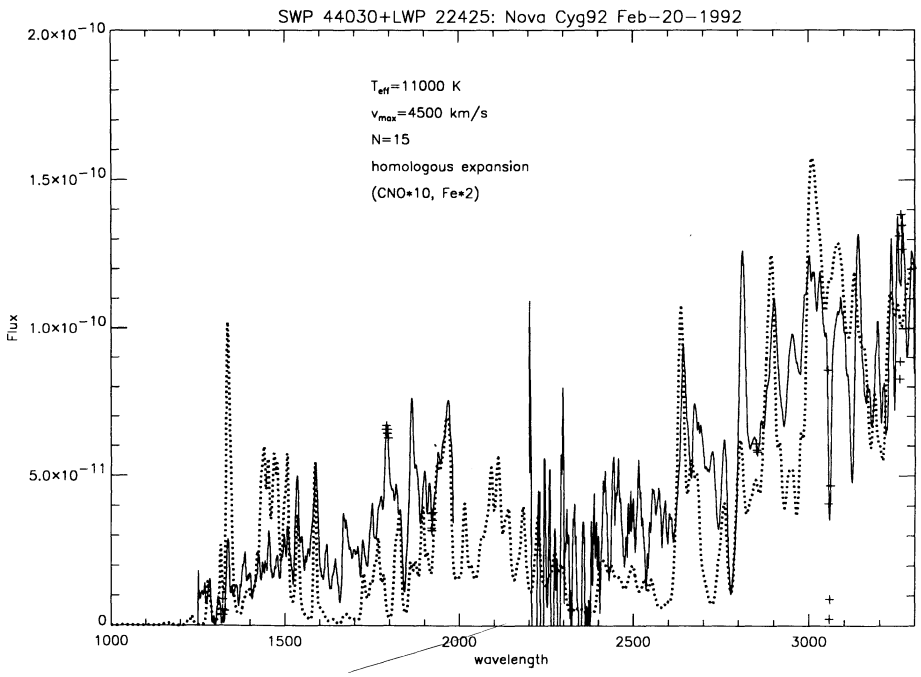

FIG. 6.—Same as Fig. 5*b*, but the abundances by number of CNO are 10 times and the Fe abundance is 2 times higher than the solar value

in the later phases, the structure of the peaks of the emission lines by a few percent when compared to the total line flux. It seems, therefore, unlikely that the absorption part of Hβ is significantly influenced by nonspherical effects only 4–5 days into outburst. The density gradient may not follow a power law in the region of Balmer line formation, because these regions tend to be very extended in nova atmospheres and could be unstable. However, this would also influence the Fe II lines and the UV spectrum, both of which are well reproduced by the model atmosphere with the power-law density. The different absorption and emission systems observed in novae are visible only in high-resolution spectra and, typically, are relatively weak as compared to the features present in the spectrum shown in Figure 8. Therefore, we conclude that the

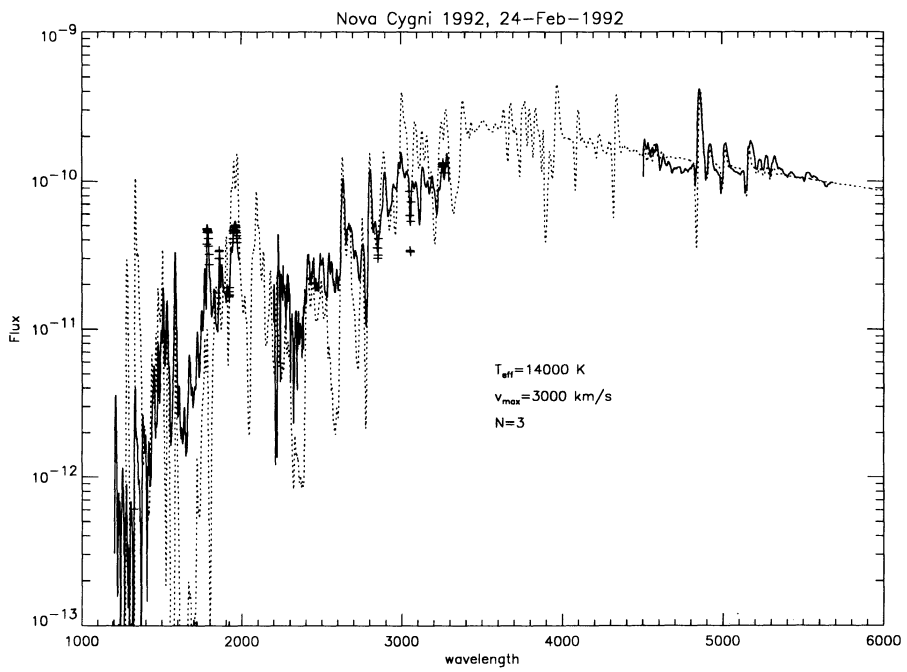

FIG. 7.—The combined optical and *IUE* spectra of NCyg92 on 1992 February 24. The dotted curve gives the best-fitting synthetic spectrum using solar abundances. The model parameters are: $T_{\rm eff}$ = 14,000 K, N = 3, $v_{\rm max}$ = 3000 km s^{-1}, constant mass-loss rate (corresponding to a linear velocity law in the case of N = 3).

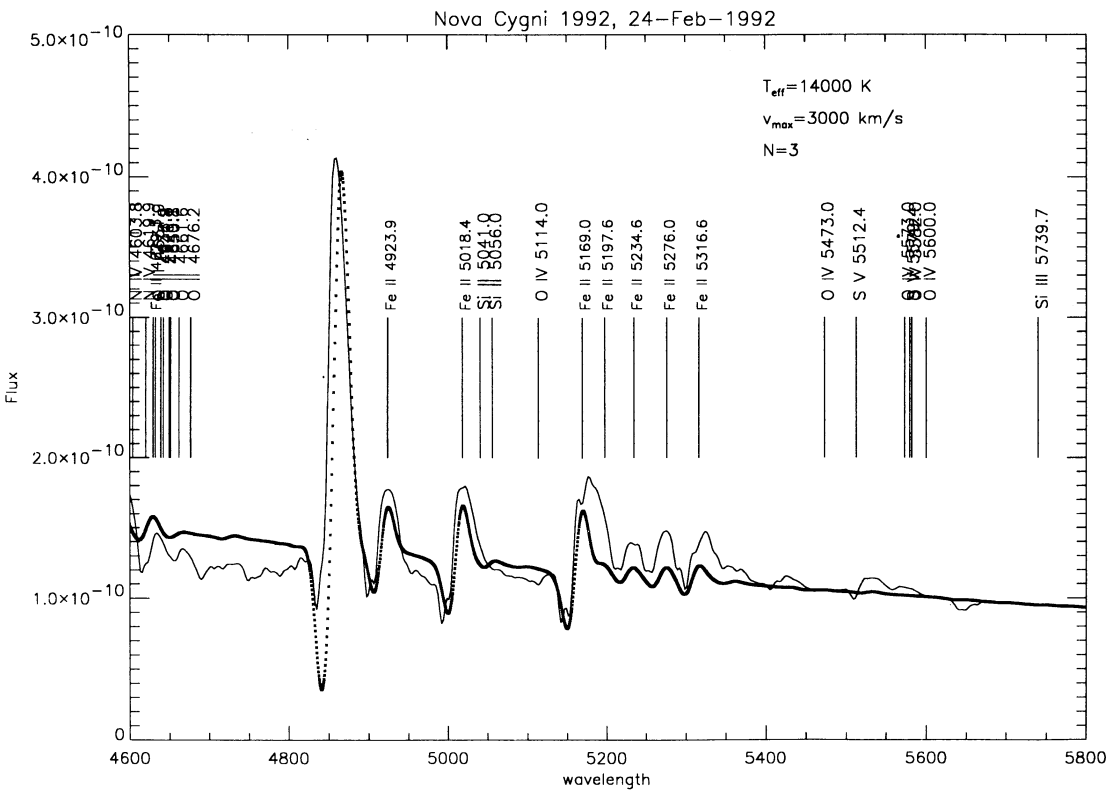

FIG. 8.—The optical spectrum of NCyg92 on 1992 February 24. The dotted curve gives the best-fitting synthetic spectrum with solar abundances. The model parameters are: $T_{\rm eff}$ = 14,000 K, N = 3, $v_{\rm max}$ = 3000 km s^{-1}, constant mass-loss rate (corresponding to a linear velocity law in the case of N = 3). For illustration, we give line identifications for the most prominent lines (other than Hβ) based on the model atmosphere. The features around 4700 Å are formed by overlapping lines of O II, Fe II, and N IV, whereas around 5600 Å lines of O IV and S V overlap.

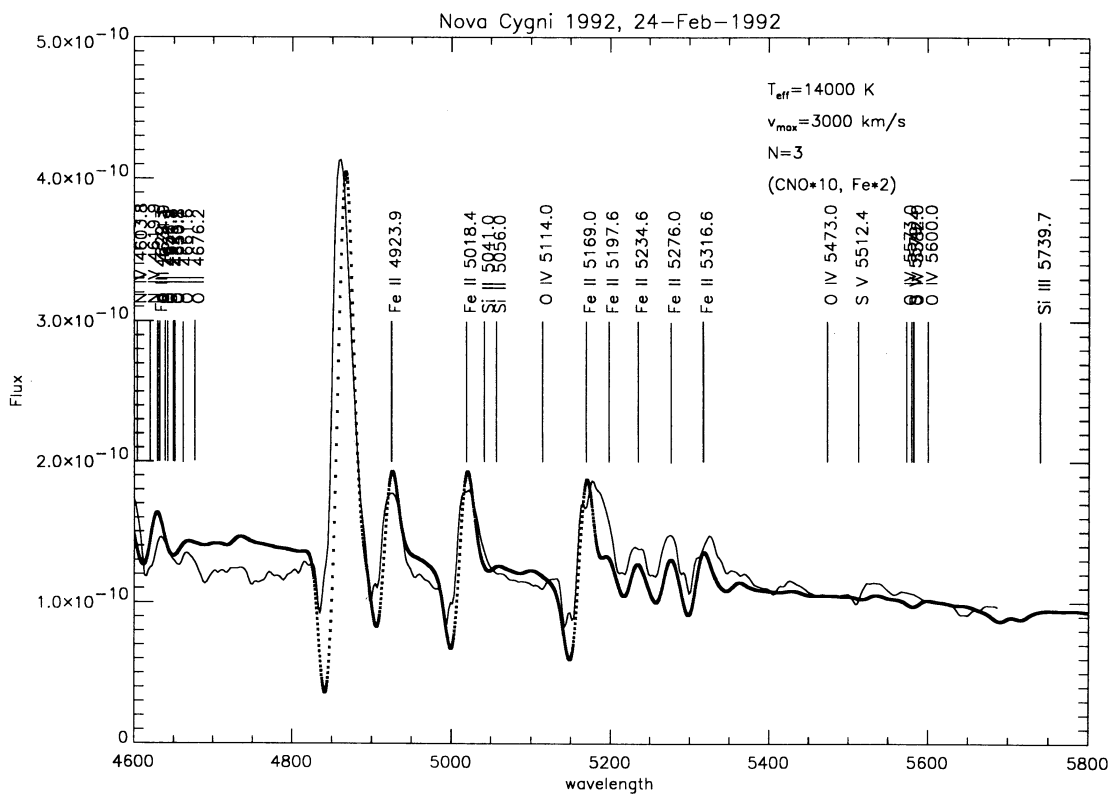

FIG. 9.—Same as for Fig. 8, but with a 2 times higher Fe/H ratio and 10 times solar CNO/H ratios (by number)

absorption part of the Hβ P Cygni profile is probably filled by emission from previously ejected material lying in the line of sight to NCyg92.

In Figures 10 and 11 we show a comparison between a high-resolution LWP *IUE* spectrum obtained on 1992 February 25 (nearly contemporaneous with the optical spectrum shown in Figs. 8 and 9) of NCyg92 with the synthetic spectrum also shown in Figure 7. In Figure 10 we label only lines other than Fe. In Figure 11 we demonstrate the effect of the many overlapping Fe II lines on the spectrum; here only the most important Fe II lines (stronger than a factor of 100 when compared to the local continuum absorption) are labeled. All labels are placed at the rest wavelength of the corresponding line. The contribution of several different ionization stages of, e.g., sulfur, is evident (Fig. 10). This is explained by the large temperature gradient present in the model atmosphere (Hauschildt et al. 1992). Even for $T_{\rm eff}$ as high as 14,000 K, the electron temperature at the outer boundary of the atmosphere is about 4000 K. At the inner boundary at $\tau_{\rm std} = 1000$ (absorption optical depth scale at 5000 Å) the electron temperatures are about 140,000 K. In addition, the continuum and line-forming regions are very extended when compared to "classical" stellar atmospheres or even supernova envelopes (see also Hauschildt et al. 1992). Therefore, we find a larger temperature gradient in the line-forming region than is found in "normal" (hydrostatic) stars and many ionization stages are present in the emitted nova spectrum.

The synthetic spectrum is able to reproduce many of the broad features found in the observed spectrum, in particular the "hole in the iron curtain" at ≈2670 Å and the Mg II $h + k$ Fe II blend. The sharp absorption features visible on top of the much broader features in the observed spectrum are not reproduced by the synthetic spectrum. These sharp features could be the UV analog of the principal absorption system frequently observed in optical nova spectra (Payne-Gaposchkin 1957). In order to produce sharp absorption features, the radial extension of this layer has to be very small and its velocity nearly constant, otherwise the lines would be broadened by the velocity dispersion and radiative transfer effects. A possible explanation is the presence of relatively sharp density peaks inside the nova shell itself, caused by instabilities in the outflow (Owocki & Rybicki 1991 and references therein). We plan to investigate this further in subsequent studies.

5. SUMMARY AND DISCUSSION

We have analyzed the early spectra of NCyg92 using our spherically symmetric, non–LTE, expanding stellar atmosphere code PHOENIX. The model atmospheres include, self-consistently, line blanketing of UV metal lines and show a number of characteristic features: (1) a very large extension of the atmosphere, typically the relative radial extension of the line and continuum forming regions is about 100; (2) large departures from LTE; (3) very large temperature gradients throughout the envelope, for example, the electron temperatures for a model with $T_{\rm eff} = 15{,}000$ K ranges from 4000 K to 150,000 K, therefore; (4) multiple ionization stages are simultaneously present in the atmosphere; (5) the early UV spectra are dominated by line-blanketing, in particular by the Fe II curtain and; (6) many of the observed "emission lines" are merely "holes in the Fe II curtain." These features distinguish the physical structure of early nova atmospheres from

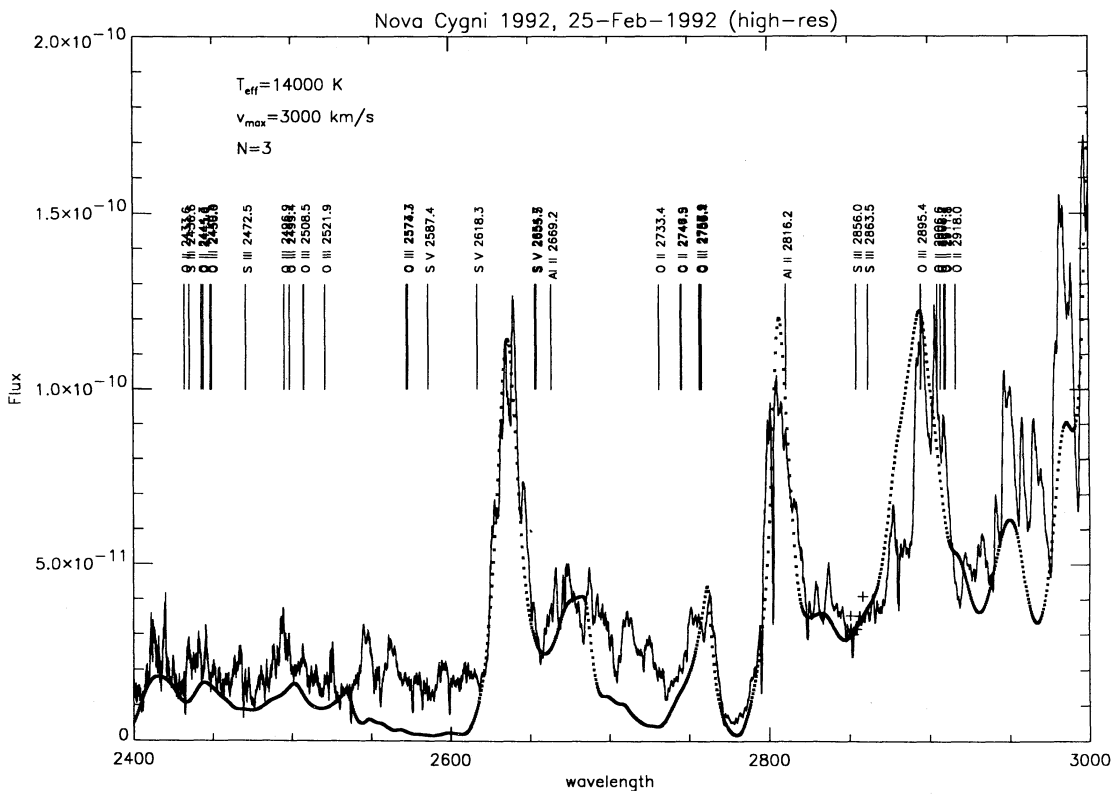

FIG. 10.—High-resolution LWR spectrum of NCy92 on 1992 February 25. The dotted line is a corresponding synthetic spectrum (solar abundances). The locations (rest wavelengths) of important lines (other than Mg II $h + k$) used in calculating the synthetic spectrum are given.

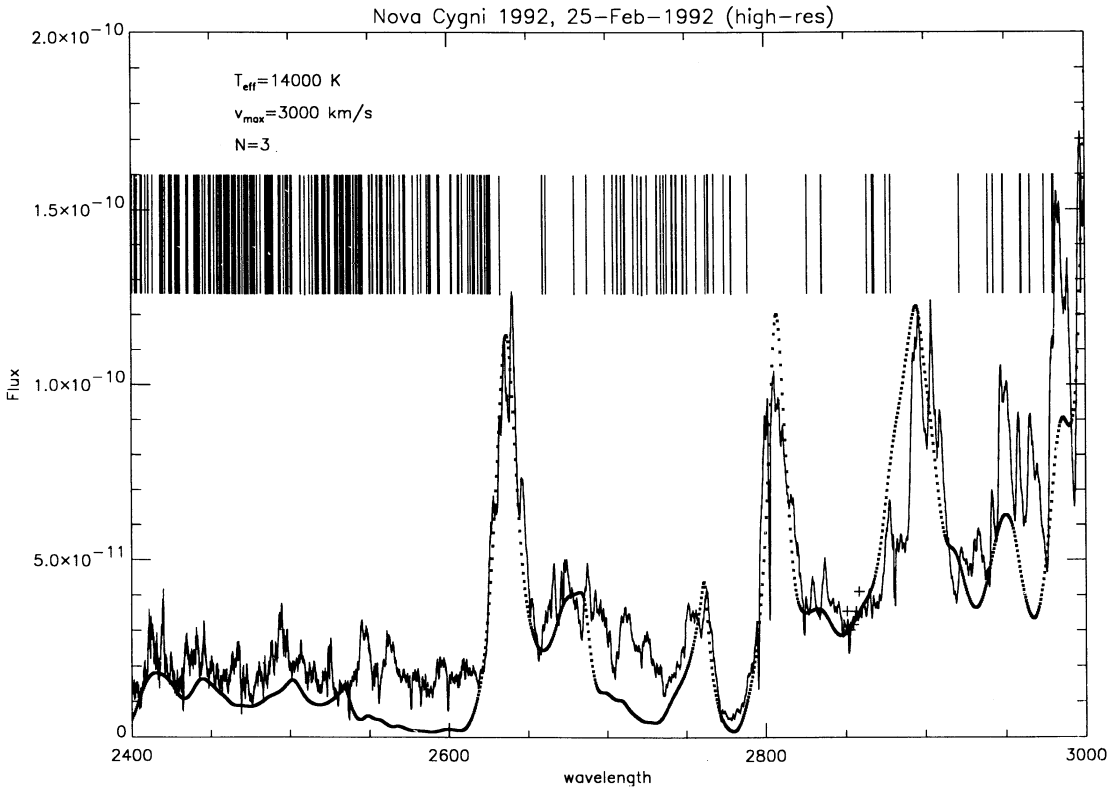

FIG. 11.—The "iron curtain" at work: same as the previous figure, but now we label only the *rest* wavelengths of Fe II lines which are stronger than a factor of 50 when compared to the local continuum. The identifications of several "emission features", which occur at "gaps in the iron curtain," is evident.

either "classical" plane parallel stellar atmospheres or supernova envelopes.

We have identified two distinct phases of spectral evolution during the early phases of the outburst of NCyg92. Our first spectrum, obtained shortly after discovery, found the expanding material in the "fireball," phase in which the spectrum forms in a very thin ($N \approx 15$), homologously expanding shell with a relatively low effective temperature $T_{\rm eff} \approx 11{,}000$ K. Because the expanding material is still very optically thick, energy from the interior cannot reach the surface and these layers continue to cool. This causes a rapid increase in the UV opacity and the emitted energy moves into the optical spectral range (due to both cooling and redistribution effects) so that the UV flux exhibits a precipitous decline. Due to the fast expansion, the luminosity and effective temperature are changing on timescales of hours. The large expansion velocities drive a rapid decline in the density so that even the increased opacity is (after a short time) insufficient to prevent the photosphere from moving inward in mass to deeper and hotter layers. This produces a shift of the energy distribution back into the UV and the energy emitted in the *IUE* spectral range recovers to its previous values. The structure of the envelope, however, has been transformed into the second, optically thick "wind" phase, which dominates the spectrum after about 4 days into the outburst. Now, in order to model the photosphere we need to use a freely expanding (linear velocity law) model atmosphere with a shallow density gradient ($N \approx 3$), a higher effective temperature, $T_{\rm eff} \approx 15{,}000$ K, and a nearly time-independent luminosity (Hauschildt et al. 1992). This picture is consistent with a radius-independent mass-loss rate for this phase of the nova outburst ($\dot{M} = \text{const.} = 4\pi r^2 \rho v$).

Our synthetic spectra are able to fit the observed spectra over a large wavelength and flux range. Most of the features in the optical as well as the *IUE* spectra are reproduced well, although the deviations are larger in the shorter wavelength range (below 1900 Å). We expect that these discrepancies can be significantly reduced if the CNO elements are treated in full non–LTE because these elements are very important opacity sources between 1300 and 1400 Å. Furthermore, we expect a better fit to the observed spectra by replacing the line list by an improved version which is now available (R. L. Kurucz 1993, private communication). These new lists will considerably improve the accuracy of the atomic data used in the spectral synthesis.

A preliminary abundance analysis has shown strong evidence for hydrogen depletion in the ejecta of NCyg92. The Fe/H ratio is about twice the solar value, and the CNO elements are probably enhanced by more than a factor of 10 as compared to solar abundances. The implied hydrogen depletion can be explained by (i) mixing of metal-rich white dwarf core material into the ejected shell during the TNR, plus (ii) burning of H to He during the TNR itself. This hydrogen depletion is required to fit even the earliest fireball spectrum, which indicates that the envelope was completely mixed, as predicted by TNR modeling. Unfortunately, there are no permitted neon lines in the wavelength region we are able to study preventing us from obtaining an abundance for that element.

The strong radiation field in the nova photosphere suggests that the velocity field may be influenced by radiation pressure. This would lead to a velocity law of the form $v = v_\infty(1 - R_*/r)^\beta$, where v_∞ is the maximum expansion velocity and R_* a reference radius (Castor, Abbott, & Klein 1975). We

will investigate this effect in detail in future studies. Note, however, that these effects will not change the basic results of the analyses we have carried out in this paper because of the small density gradient and large extension of the nova photosphere.

We are very grateful to G. C. Anupama, E. Baron, L. Ensman, R. Gonzales-Riestra, J. Krautter, G. Shaviv, W. Sparks, J. Truran, and R. Wehrse for discussions about novae and their spectra and to the referee, S. Owocki, for his helpful comments on an earlier draft of this paper. We thank B. Peterson and R. Bertram for assisting in obtaining the optical spectrum of 1992 February 24. S. Starrfield and P. Hauschildt acknowledge partial support from a NASA LTSA grant to ASU and S. Starrfield also acknowledges NSF and NASA *IUE* grants to ASU.

REFERENCES

Baschek, B., Scholz, M., & Wehrse, R. 1991, A&A, 288, 374
Castor, J. D., Abbott, D., & Klein, R. 1975, ApJ, 195, 157
Collins, M. 1992, IAU Circ. No. 5454
Hauschildt, P. H. 1992a, J. Quant. Spectrosc. Rad. Transf., 47, 433
———. 1992b, ApJ, 398, 224
———. 1993, J. Quant. Spectrosc. Rad. Transf., 50, 301
Hauschildt, P. H., & Wehrse, R. 1991, J. Quant. Spectrosc. Rad. Transf., 46, 81
Hauschildt, P. H., Wehrse, R., Starrfield, S., & Shaviv, G. 1992, ApJ, 393, 307
Kurucz, R. L. 1988, private communication
Kurucz, R. L., & Peytremann, E. 1975, Smithsonian Astrophys. Obs. Spec. Rep. 362
Mikuz, A. 1992, IAU Circ., 5457
Mihalas, D. 1978, Stellar Atmospheres (San Francisco: Freeman)
Owocki, S. P., & Rybicki, G. B. 1991, ApJ, 368, 261
Payne-Gaposchkin, C. 1957, The Galactic Novae (Amsterdam: North-Holland)
Saizar, P., et al. 1992, ApJ, 398, 651
Shore, S. N., Sonneborn, G., Starrfield, S., Gonzales-Riestra, R., & Ake, T. 1994, ApJ, in press
Shore, S. N., Sonneborn, G., Starrfield, S., Gonzales-Riestra, R., & Polidan, R. S. 1993, AJ, in press
Starrfield, S. 1989, in Classical Novae, ed. M. Bode & A. Evans (New York: Wiley), 39
Wagner, R. M. 1992, in Astronomical CCD Observing and Reduction Techniques, ed. S. B. Howell (ASP Conf., 23), (San Francisco: ASP), 160